Chemistry–A European Journal
Research Article
doi.org/10.1002/chem.202200626
Chemistry Europe
European Chemical Societies Publishing
www.chemeurj.org

Reactivity of Xantphos-Type Rhodium Complexes Towards SF_4: SF_3 Versus SF_2 Complex Generation

Martin Wozniak,[a] Stefan Sander,[a] Beatrice Cula,[a] Mike Ahrens,[a] and Thomas Braun*[a]

Abstract: S–F-bond activation of sulfur tetrafluoride at [Rh(Cl)($^{t\text{Bu}}$xanPOP)] (**1**; $^{t\text{Bu}}$xanPOP = 9,9-dimethyl-4,5-bis-(di-tert-butylphosphino)-xanthene) led to the formation of the cationic complex [Rh(F)(Cl)(SF_2)($^{t\text{Bu}}$xanPOP)][SF_5] (**2a**) together with *trans*-[Rh(Cl)(F)$_2$($^{t\text{Bu}}$xanPOP)] (**3**) and *cis*-[Rh(Cl)$_2$(F)($^{t\text{Bu}}$xanPOP)] (**4**) which both could also be obtained by the reaction of SF_5Cl with **1**. In contrast to that, the conversion of SF_4 at the methyl complex [Rh(Me)($^{t\text{Bu}}$xanPOP)] (**5**) gave the isolable and room-temperature stable cationic λ^4-trifluorosulfanyl complex [Rh(Me)(SF_3)($^{t\text{Bu}}$xanPOP)][SF_5] (**6**). Treatment of **6** with the Lewis acids BF_3 or AsF_5 produced the dicationic difluorosulfanyl complex [Rh(Me)(SF_2)($^{t\text{Bu}}$xanPOP)][BF_4]$_2$ (**8a**) or [Rh(Me)(SF_2)($^{t\text{Bu}}$xanPOP)][AsF_6]$_2$ (**8b**), respectively. Refluorination of **8a** was possible with the use of dimethylamine giving [Rh(Me)(SF_3)($^{t\text{Bu}}$xanPOP)][BF_4] (**9**). A reaction of **6** with trichloroisocyanuric acid (TClCA) gave the fluorido complex [Rh(F)(Cl)(SF_2)($^{t\text{Bu}}$xanPOP)][Cl] (**2b**) together with chloromethane and SF_5Cl.

Introduction

Due to the high significance of fluorine containing organic building blocks in materials sciences, agricultural and pharmaceutical chemistry, their formation has gained in importance for the last half a century.[1] However, the selective introduction of fluorine atoms into organic molecules remains a challenging task. Methods for fluorination include the deoxyfluorination of carbonyl compounds or alcohols on using sulfur tetrafluoride.[2] The latter gas is highly toxic, and its handling can be difficult. Hence, more convenient and commercially available SF_4 derivatives such as diethylaminosulfur trifluoride (DAST), Deoxo-Fluor® or Fluolead™ have been developed.[2c,3] Transition metal derivatives of SF_4 have also been reported, but studies on their reactivity are rather rare. SF_3 fluorosulfanyl complexes have been characterized spectroscopically for platinum, rhodium and iridium, only.[4] The determination of structures in the solid state by X-ray diffraction was, so far, not described. Holloway and Ebsworth et al. reported on S–F bond oxidative addition reactions of SF_4 at Vaska-type complexes of rhodium and iridium to give [MX(F)(SF_3)(CO)(PEt_3)$_2$] (M = Rh, Ir; X = Cl, Br, I, NCO, NCS). In the case of the rhodium compounds the reactions were unselective and the products were not stable.[4a,b,d] A selective oxidative addition was achieved by the Braun group to yield *cis,trans*-[Rh(F)$_2$(SF_3)(CO)(PEt_3)$_2$], but again the complex is unstable and could not be isolated.[4b,g] Another interesting approach includes the synthesis of *trans*-[Pt(F)(SF_3)(PCy_3)$_2$] either by reaction of [Pt(PCy_3)$_2$] with SF_4 or by activation of SF_6. In reactivity studies the deoxyfluorination of ethanol and benzophenone was achieved.[4e,f,k]

Herein we report on the reactivity of $^{t\text{Bu}}$xanPOP type ($^{t\text{Bu}}$xanPOP = 9,9-dimethyl-4,5-bis-(di-tert-butylphosphino)-xanthene) Rh(I) complexes towards SF_4 to yield either an SF_2 or SF_3 complex. An unusually stable cationic Rh^{III}–SF_3 compound [Rh(Me)(SF_3)($^{t\text{Bu}}$xanPOP)][SF_5] (**6**) was isolated and characterized crystallographically. Reactions of **6** with a Lewis acid or trichloroisocyanuric acid (TClCA) result in the generation of SF_2 complexes.

Results and Discussion

Reactivity of [Rh(Cl)($^{t\text{Bu}}$xanPOP)] (1) towards SF_4

A reaction of [Rh(Cl)($^{t\text{Bu}}$xanPOP)] (**1**) with two equivalents of SF_4 gave the cationic complex [Rh(F)(Cl)(SF_2)($^{t\text{Bu}}$xanPOP)][SF_5] (**2a**) as well as *trans*-[Rh(Cl)(F)$_2$($^{t\text{Bu}}$xanPOP)] (**3**), *cis*-[Rh(Cl)$_2$(F)($^{t\text{Bu}}$xanPOP)] (**4**) and three unknown Rh complexes in a ratio of 1:0.5:1.5:0.2:0.2:0.1 (based on $^{31}P\{^1H\}$ NMR data, Scheme 1). Mechanistically, the generation of **2a** might proceed via an initial oxidative addition at **1**, followed by a fluoride abstraction by an additional molecule of SF_4 to give the SF_5^- anion. A subsequent fluoride migration from the SF_3 ligand to the metal center results in the generation of **2a**.

The complexes **3** and **4** were also obtained independently in ratio of 0.2:1 by treatment of **1** with an excess of SF_5Cl in toluene (Scheme 1). It can be assumed that the conversion involves a formation of SF_4, which in turn can result in the generation of **4** by fluorination, although the fate of the sulfur

[a] M. Wozniak, S. Sander, Dr. B. Cula, Dr. M. Ahrens, Prof. Dr. T. Braun
Department of Chemistry
Humboldt-Universität zu Berlin
Brook-Taylor-Str. 2, 12489 Berlin (Germany)
E-mail: thomas.braun@cms.hu-berlin.de

Supporting information for this article is available on the WWW under https://doi.org/10.1002/chem.202200626

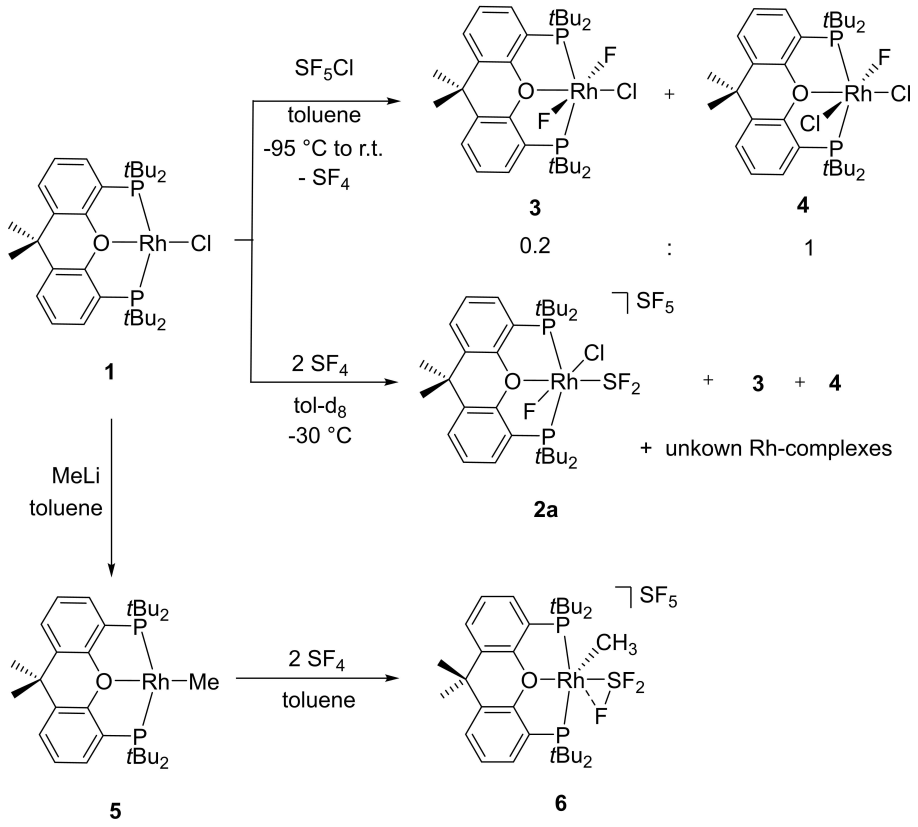

Scheme 1. Formation of [Rh(F)(Cl)(SF_2)(^{tBu}xanPOP)][SF_5] (**2a**), *trans*-[Rh(Cl)$(F)_2$(^{tBu}xanPOP)] (**3**) and *cis*-[Rh$(Cl)_2$(F)(^{tBu}xanPOP)] (**4**)

is unclear.[4,5] A formation of a sulfanyl complex was not observed.

The NMR data of the cation in **2a** are described below. A signal at $\delta = 61.2$ ppm in the ^{19}F NMR spectrum can be assigned to the SF_5^- anion.[4h,6] In the ^{19}F NMR spectrum of **3** the fluorido ligands give a broad doublet at characteristic high field $\delta = -537.6$ ppm with couplings to rhodium ($^1J_{F,Rh} = 239$ Hz) and both phosphorus atoms ($^2J_{F,P} = 11$ Hz).[7] The $^{31}P\{^1H\}$ NMR spectrum displays a doublet of triplets resulting from couplings to rhodium and both fluorido ligands ($^1J_{P,Rh} = 90$ Hz, $^2J_{P,F} = 11$ Hz) at $\delta = 42.0$ ppm with the coupling constant $^2J_{P,F}$ being typical for a *trans*-complex.[8] Suitable crystals for structure determination of **3** in the solid state could be obtained from a solution of the reaction mixture in tetrahydrofuran (see Supporting Information, Figure S36 and Table S2). The $^{31}P\{^1H\}$ NMR spectrum of **4** shows a doublet of doublets $\delta = 41.5$ ppm with couplings to rhodium ($^1J_{P,Rh} = 87$ Hz) and to the fluorido ligand ($^2J_{P,F} = 11$ Hz). The resonance of the fluorido ligand at $\delta = -472.4$ ppm in the ^{19}F NMR spectrum shows a broad doublet pattern resulting from the coupling to the metal center ($^2J_{F,Rh} = 220$ Hz). Suitable crystals for structure determination of **4** in the solid state were obtained from the reaction solution (see Supporting Information, Figure S37 and Table S2). The molecular structure in the solid state confirms the *cis* arrangement of the chlorido ligands.

Conversion of [Rh(Me)(^{tBu}xanPOP)] (5) into a cationic λ^4-trifluorosulfanyl Rh^{III} complex

To assess the influence of the anionic ligand on the reactivity towards SF_4, the methyl complex [Rh(Me)(^{tBu}xanPOP)] (**5**) was synthesized. It can be speculated that a better σ-donor ligand would hamper fluoride migration from a putative SF_3 ligand to the metal. The starting compound, complex **5**, was obtained by treatment of [Rh(Cl)(^{tBu}xanPOP)] (**1**) with MeLi. (Scheme 1). The isotopologue [Rh($^{13}CH_3$)(^{tBu}xanPOP)] (**5′**) is accessible accordingly by a reaction of **1** with ^{13}C labeled MeLi. The $^{31}P\{^1H\}$ NMR spectrum of **5** exhibits a doublet at $\delta = 50.5$ ppm for the phosphine atoms of the ^{tBu}xanPOP pincer ligand with a coupling constant of $^1J_{P,Rh} = 177$ Hz. This value is in a typical range of other literature known xantphos-type rhodium complexes in the oxidation state +I.[8,9] The signal for the methyl ligand in the ^1H NMR spectrum of **5** appears at 0.53 ppm as a triplet of doublets due to couplings to phosphorus and rhodium ($^3J_{H,P} = 5.7$ Hz and $^2J_{H,Rh} = 2.9$ Hz). The isotopologue **5′** shows additional doublet couplings in the $^{31}P\{^1H\}$ NMR spectrum of $^2J_{P,C} = 11$ Hz and in the ^1H NMR spectrum of $^1J_{H,C} = 122.8$ Hz. The $^{13}C\{^1H\}$ NMR spectrum displays a doublet of triplets at $\delta = -21.7$ ppm for the methyl ligand ($^1J_{C,Rh} = 34$ Hz and $^2J_{C,P} = 11$ Hz).

Red crystals suitable for single X-ray crystallography of **5** were obtained by recrystallization from methylcyclohexane (Figure 1). The structure of **5** reveals a distorted square-planar coordination geometry at the metal center in which both

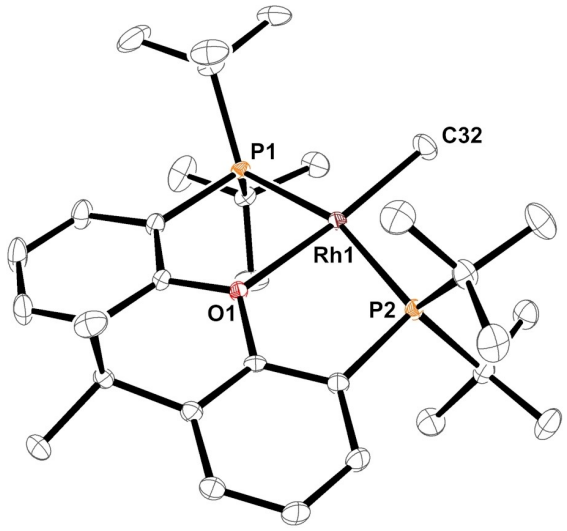

Figure 1. Molecular structure of **5** (ORTEP, ellipsoids are set at 50% probability. All hydrogen atoms are omitted for clarity. Selected distances [Å] and bond angles [°]: Rh1–P1 2.2678(3), Rh1–P2 2.2495(3), Rh1–O1 2.2210(9), Rh1–C32 2.0651(13); P1–Rh1–P2 161.618(12), C32–Rh1–O1 171.52(5), C32–Rh1–P1 98.21(4), C32–Rh1–P2 98.02(4), P1–Rh1–O1 82.95(2), P2–Rh1–O1 82.28(2).

phosphorus atoms of the $^{t\text{Bu}}$xanPOP ligand are located in a mutually *trans*-position. The Rh–P bond lengths (2.2678(3) Å and 2.2495(3) Å) are in good accordance to the data for literature known Rh$^{\text{I}}$-complexes bearing $^{t\text{Bu}}$xanPOP ligands, as **1** for instance.[9a] In contrast to this, the Rh–O bond length (2.2210(9) Å) in **5** is significantly shorter than the one in **1** and is comparable to the corresponding distance in alkenyl xantphos-type rhodium complexes.[9f] The angles P1–Rh1–P2 (161.618(12)°) and C32–Rh1–O1 (171.52(5)°) mirror clearly the distorted square-planar geometry.

Treatment of a dark red CD_2Cl_2 solution of complex **5** with two equivalents of SF_4 at room temperature led to the formation of the ionic λ^4-trifluorosulfanyl complex [Rh(Me)(SF_3)($^{t\text{Bu}}$xanPOP)][SF_5] (**6**) together with the difluorido complex *trans*-[Rh(Me)$(F)_2$($^{t\text{Bu}}$xanPOP)] (**7**) and four unknown rhodium products in a ratio of 1:1.2:0.3:0.3:0.8:0.6 (based on ^{31}P{^{1}H} NMR). When this reaction was performed in toluene-d_8 at 193 K, a decolorization of the reaction solution took place, and a subsequent precipitation of **6** as green crystals occurred, which were separated from the product mixture (isolated yield: 82%, Scheme 1). The ^{31}P{^{1}H} NMR spectrum of the overlaying reaction solution revealed the presence of **7** together with several rhodium compounds in minor amounts. [Rh($^{13}CH_3$)(SF_3)($^{t\text{Bu}}$xanPOP)][SF_5] (**6′**) was prepared in a similar manner starting from **5′**. Unlike found for most of the literature-known SF_5 salts, the anion in **6** does not decompose to SF_4 and fluoride when **6** is stored at room temperature under an argon atmosphere.[4h,6,10]

Mechanistically, it can be assumed that an oxidative addition of SF_4 at **1** yields initially [Rh(Me)(F)(SF_3)($^{t\text{Bu}}$xanPOP)]. The latter reacts with a second equivalent of SF_4 to give after fluoride abstraction **6** bearing the SF_5^- anion. A comparable reactivity pattern was described by Murdoch and coworkers with TeF_4. Treatment of *trans*-[Rh(Cl)(CO)$(PEt_3)_2$] with two equivalents of TeF_4 resulted in the formation of *trans*-[Rh(Cl)(CO)$(PEt_3)_2$(TeF_3)][TeF_5].[4d]

The crystals of **6** were studied by single X-ray crystallography (Figure 2). Note that structural data of a λ^4-trifluorosulfanyl complex in the solid state were not reported before. There is a disorder of the metal bound sulfur atom S1 and the equatorial fluorine atom F3 with an occupancy of 0.44:0.56 (see Supporting Information, Figure S38). The SF_5^- anion of **6** shows an average S–$F_{equatorial}$ bond length of 1.72 Å and S–F_{axial} bond length of 1.580(3) Å, which is similar to data found for other solid-state structures reported for this anion.[6a,10a–d] The structure of the cationic part in **6** exhibits a slightly distorted square-pyramidal coordination geometry at the rhodium atom with the λ^4-trifluorosulfanyl ligand located in a *trans* position to the ether function of the phosphine with O1–Rh1–S1a and O1–Rh1–S1b angles of 169.78(17)° and 170.6(2)°, respectively. The Rh–S bond lengths (Rh1–S1a 2.195(9) Å, Rh1–S1b 2.164(11) Å) are significantly smaller when compared to the one in [Rh(SH)($^{t\text{Bu}}$xanPOP)] (Rh–S 2.2865(4) Å or in various cationic xantphos-type Rh$^{(\text{III})}$–S complexes as for instance [Rh(xanPOP)(C_6H_4COMe)(SMe)][$BAr^F{}_4$] (Rh–S 2.3373(14) Å, xanPOP = 4,5-bis(diphenylphosphino)-9,9-dimethylxanthene, Ar^F = 3,5-$(CF_3)_2C_6H_3$).[8,11] The SF_3 ligand displays an Rh···F interaction of 2.418(3) Å, which results in a small F1–S1a–Rh angle of 72.3(3)° as well as the significantly elongated bond between the sulfur atom and the fluorine atom F1 of 1.880(7) Å.

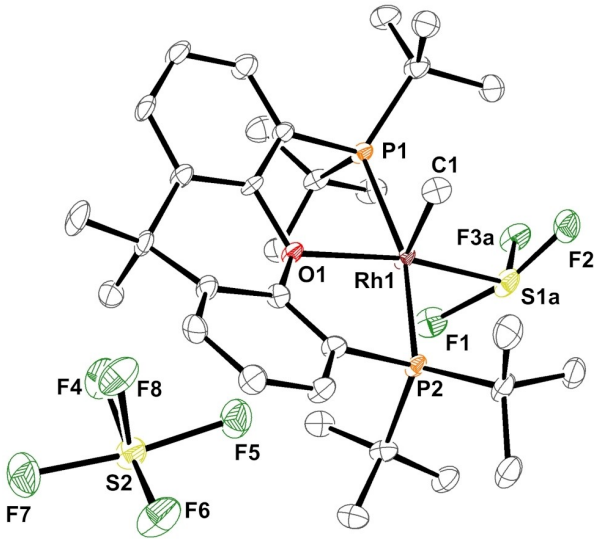

Figure 2. Molecular structure of **6** (ORTEP, ellipsoids are set at 50% probability. All hydrogen atoms are omitted for clarity. Selected distances [Å] and bond angles [°]: Rh1–P1 2.3999(12), Rh1–P2 2.3939(11), Rh1–O1 2.220(3), Rh1–C1 2.070(5), Rh1–S1a 2.195(9), Rh1–F1 2.418(3), S1a–F1 1.880(7), S1a–F2 1.680(7), S1a–F3a 1.585(8), S2–F8 1.580(3), S2–F7 1.705(3), S2–F6 1.712(3), S2–F5 1.727(3), S2–F4 1.728(3); P1–Rh1–P2 163.79(4), S1a–Rh1–O1 169.78(17), C1–Rh1–O1 84.14(16), C1–Rh1–P1 88.92(14), C1–Rh1–P2 88.88(14), C1–Rh1–S1a 104.2(2), P1–Rh1–O1 82.13(8), P2–Rh1–O1 81.67(8), S1a–Rh1–P1 103.63(8), S1a–Rh1–P2 92.48(14), F1–S1a–Rh1 72.3(3), F2–S1a–Rh1 102.0(4), F3a–S1a–Rh1 113.3(4), F3a–S1a–F1 82.3(4), F3a–S1a–F2 88.1(4).

At 193 K the $^{31}P\{^1H\}$ NMR spectrum of **6** displays an AB pattern, which was simulated (Figure 3). The inequivalent phosphorus atoms P_a and P_b couple to rhodium ($^1J_{Pa,Rh}$ = 103.3 Hz, P_b: $^1J_{Pb,Rh}$ = 95.5 Hz),[9a,11,12] to each other ($^2J_{Pa,Pb}$ = 292.0 Hz)[4a,b,i,12b,13] and to one of the three sulfur bound fluorine atoms, with coupling constants $^3J_{Pa,Fa'}$ = 28.4 Hz and $^3J_{Pb,Fa'}$ = 37.1 Hz. The signal in the $^{13}C\{^1H\}$ NMR spectrum of **6** at δ = 7.8 ppm is significantly low-field shifted by about 28 ppm when compared to the corresponding resonance for **5**. It appears as a doublet of multiplets with $^1J_{C,Rh}$ = 30 Hz.

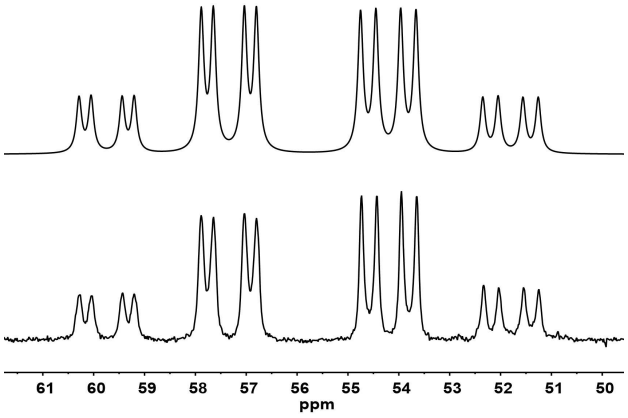

Figure 3. Experimental (bottom) and simulated (top) $^{31}P\{^1H\}$ NMR spectra of [Rh(Me)(SF_3)(^{tBu}xanPOP)][SF_5] (**6**) at 193 K with the following shifts and coupling constants obtained from the simulated spectrum: δ = 58.3 ppm ($^1J_{Pa,Rh}$ = 103.3 Hz, $^2J_{Pa,Pb}$ = 292.0 Hz, $^3J_{Pa,Fa'}$ = 28.4 Hz, P_a), 53.3 ($^1J_{Pb,Rh}$ = 95.5 Hz, $^2J_{Pb,Pa}$ = 292.0 Hz, $^3J_{Pb,Fa'}$ = 37.1 Hz, P_b).

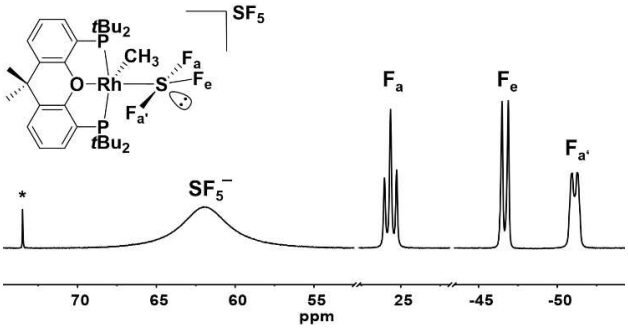

Figure 4. ^{19}F NMR spectrum of [Rh(Me)(SF_3)(^{tBu}xanPOP)][SF_5] (**6**) at 195 K. *SOF_2

The ^{19}F NMR spectrum of **6** at 193 K (Figure 4) shows one broad signal at δ = 62.2 ppm for the SF_5^- anion[4h,6,10b,c,e] and three signals with an integral ratio of 1:1:1 for each fluorine atom of the λ^4-trifluorosulfanyl ligand at δ = 25.6 (F_a), −46.7 (F_e) and −51.1 ppm ($F_{a'}$). Compared to the NMR data of literature known SF_3 compounds the signals for F_a and $F_{a'}$ are significantly shifted to higher field. However, an additional interaction of a S–F moiety with the rhodium center has only been identified for **6**, and the dissimilar NMR data suggest that this interaction also persists in solution at 193 K. No apparent coupling is observed between $F_{a'}$ and F_e neither in the ^{19}F NMR spectrum nor in the corresponding $^{19}F,^{19}F$-COSY NMR spectrum (Supporting Information, Figure S16).

A multiplication of the FID with a Gaussian function reveals several coupling constants. Simulation of the signal at δ = −51.1 ppm ($F_{a'}$) gives coupling constants for the couplings to one sulfur bound fluorine atom $^2J_{Fa',Fa}$ = 104.9 Hz, to the metal center of $J_{Fa',Rh}$ = 21.1 Hz, as well as to both phosphorus atoms with $^3J_{Fa',Pa}$ = 30.2 Hz and $^3J_{Fa',Pb}$ = 35.9 Hz. The latter values are in good agreement with data from the simulation of the $^{31}P\{^1H\}$ NMR spectrum (see Figure 3).

Variable-temperature ^{31}P and ^{19}F NMR studies of **6** were performed (Figure 5). At 193 K the ^{31}P NMR spectrum reveals two signals for the inequivalent phosphorus atoms which coalesce to one signal with a doublet of multiplets pattern at 298 K. In the ^{19}F NMR spectra the signals at δ = 25.6 and −51.1 ppm for the axial fluorine atoms F_a and $F_{a'}$ broaden above 193 K. Simultaneously all three signals converge into the resonance assigned to F_e resulting in a triplet like pattern above 253 K. An integration against an external standard confirms that three fluorine atoms can be assigned to the latter signal. These observations are consistent with the conversion of the low-temperature conformation of **3** into a structure, which does not exhibit a Rh···F interaction and the three fluorine atoms bound

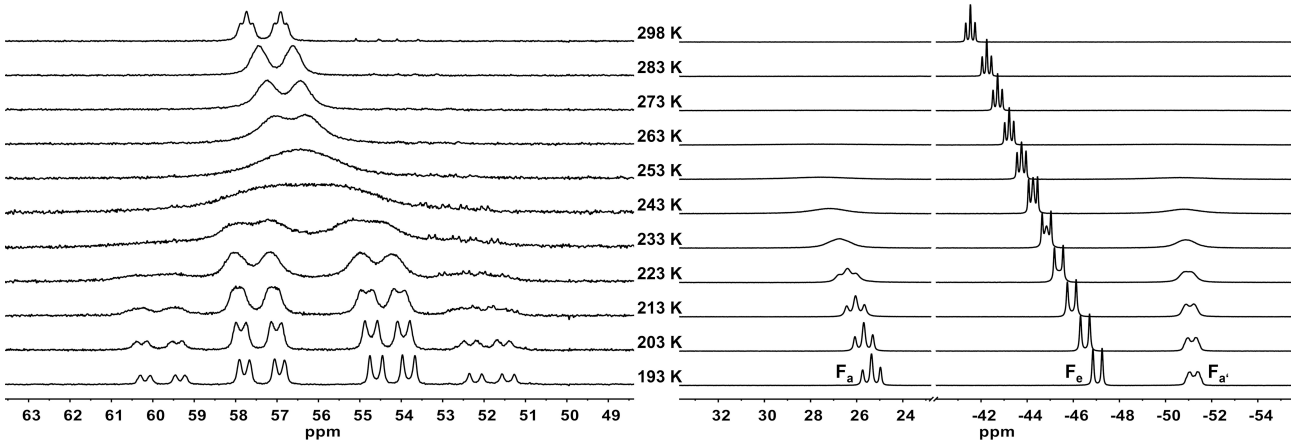

Figure 5. $^{31}P\{^1H\}$ NMR (121.5 MHz, left) and sections of ^{19}F NMR spectra (282.5 MHz, right) of **6** recorded at different temperatures ranging from 193 K to 298 K.

to sulfur exchange on the NMR time-scale. However, it is intriguing that the resulting signal at $\delta = -42$ ppm at 298 K seems to develop from the resonance for F_e. We suggest that a fluxional structure at room temperature must resemble considerably the environment of F_e. Tentatively, the fluxional structure might adopt a trigonal bipyramidal configuration at sulfur with the free electron pair in the axial position, or a (distorted) trigonal pyramidal structure with Rh at the apical position.

To get a further insight into the structure of **6**, DFT calculations were performed (Figure 6). The calculated minimum structure of the cation in vacuum is largely in agreement with the data obtained from single X-ray crystallography. The Rh–S–F angle of 70.06° as well as the Rh–F distance (2.3825 Å) and the S–F bond length (1.9338 Å) mirror the Rh···F interaction. The absence of a bond critical point in an AIM analysis and an only moderate Wiberg bond index suggests that the interaction between the sulfur bound fluoride and the metal center has no significant covalent contribution. Moreover, a relaxed scan of the potential energy surface was performed with gradual changes of the F–S–Rh angle in 5-degree steps (see Supporting Information). The gradual change of the angle resembles a pathway for a putative migration of a fluoride from the SF_3 ligand to the metal center to give a SF_2 fluorido complex. The scan confirms that the structure determined in vacuum indeed represents the energetic minimum.

The NBO analysis of the frontier orbitals of **6** suggests the presence of a stereoactive electron lone pair at the sulfur atom, which is in accordance with the literature on DFT calculations of other λ^4-trifluorosulfanyl complexes (HOMO-4, Supporting Information: Figure S42).[4e,g,i,5]

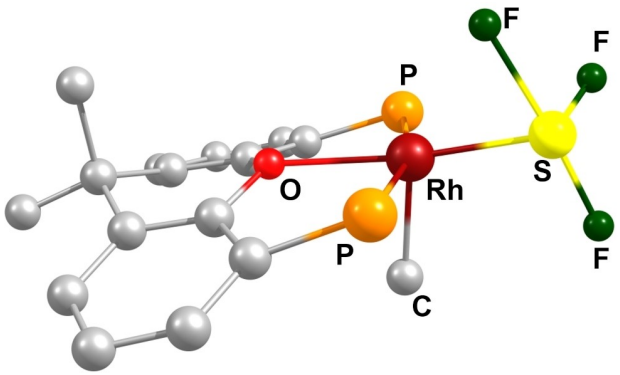

Figure 6. DFT-optimized structure of the cationic part of **6**; all hydrogen atoms as well as the *tert*-butyl groups at the phosphorus atoms have been omitted for clarity. B3LYP/cc-pvtz with Grimme D3 dispersion correction including Becke-Jones damping (RECP with corresponding cc-pvdz basis set for Rh).

Reactivity of [Rh(Me)(SF_3)(^{tBu}xanPOP)][SF_5] (3) towards Lewis acids and trichloroisocyanuric acid (TClCA)

Remarkably, treatment of **6** with BF_3 in a 2:1 molar ratio led to the generation of the unique dicationic SF_2 complex [Rh(Me)(SF_2)(^{tBu}xanPOP)][BF_4]$_2$ as well as of SF_4 (**8a**, Scheme 2). [Rh($^{13}CH_3$)(SF_2)(^{tBu}xanPOP)][BF_4]$_2$ (**8a'**) was generated in a similar manner starting from **6'**. Likewise, a reaction of **6** with arsenic pentafluoride gave [Rh(Me)(SF_2)(^{tBu}xanPOP)][AsF_6]$_2$ (**8b**), which slowly crystallized in dichloromethane (Scheme 2). Lewis-acid induced fluoride abstraction reactions from SF_3 ligands were reported before at *trans*-[Ir(X)(F)(SF_3)(CO)(PEt_3)$_2$] (X = Cl, F) and *trans*-[Pt(F)(SF_3)(PR_3)$_2$] (R = iPr, Cy), but in these cases monocationic complexes were formed.[4a,e,i]

Adding an excess of dimethylamine to the reaction mixture containing [Rh(Me)(SF_2)(^{tBu}xanPOP)][BF_4]$_2$ (**8a**) resulted in the regeneration of compound [Rh(Me)(SF_3)(^{tBu}xanPOP)][BF_4] (**9**, Scheme 2). Apparently the BF_4^- anion acts as the fluoride source. In contrast to the reported refluorination reactions at *trans*-[Ir(Cl)(F)(SF_2)(CO)(PEt_3)$_2$][BF_4] by treatment with $NHMe_2$, the adduct BF_3·$NHMe_2$ was not detected, presumably because of the presence of SF_4. Note, that the complex **8b** is fairly stable in vacuum but decomposes after treatment with dimethylamine (to unknown products).

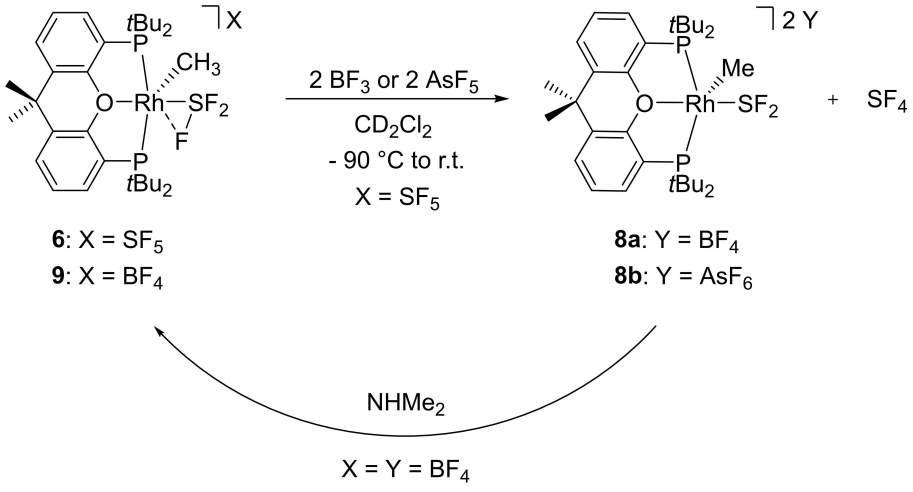

Scheme 2. Formation of the dicationic SF_2 complexes [Rh(Me)(SF_2)(^{tBu}xanPOP)][BF_4]$_2$ (**8a**) and [Rh(Me)(SF_2)(^{tBu}xanPOP)][AsF_6]$_2$ (**8b**) and dimethylamine-induced refluorination of **8a** to get [Rh(Me)(SF_3)(^{tBu}xanPOP)][BF_4] (**9**).

Treatment of the reaction mixture containing [Rh(F)(Cl)(SF_2)(^{tBu}xanPOP)][SF_5] (**2a**) with an excess of BF_3 did not lead to an abstraction of the fluorido ligand and the generation of a dication, but merely to an anion exchange at **2a** of SF_5^- to BF_4^- to give [Rh(F)(Cl)(SF_2)(^{tBu}xanPOP)][BF_4] (**2c**) with a simultaneous formation of SF_4, which was detected in the ^{19}F NMR spectrum of the reaction mixture.

At room temperature the ^{31}P{^{1}H} NMR spectrum of the green reaction mixture containing **8a** shows a doublet of triplets at $\delta = 65.5$ with couplings to rhodium of $^1J_{P,Rh} = 87$ Hz and to both fluorine atoms of the SF_2 ligand with a coupling constant of $^3J_{P,F} = 27$ Hz. The latter coupling constant is in accordance with couplings to an SF_2 ligand bound to a transition metal center.[4a,e,f,i] At 203 K the ^{19}F NMR spectrum shows four resonances at $\delta = 86.5$, 34.0, −31.6 and −149.0 ppm with an integral ratio of 2:2:2:8. The signal at high field can be assigned to the BF_4^- anions.[14] The two broad low-field shifted signals correspond to resonances of SF_4, which is presumably generated by fluoride abstraction from the SF_5 anion in **6**.[15] The SF_2 ligand can be assigned to the broad triplet at $\delta = -31.6$ ppm, which is in a typical range for SF_2 ligands.[4a,e,f,i] Upon heating up to room temperature the signal sharpens to a triplet of doublets with coupling constants $^3J_{F,P} = 27$ Hz and $^2J_{F,Rh} = 8$ Hz. The ^{13}C{^{1}H} NMR spectrum of **8a'** shows a doublet at $\delta = 32.4$ ppm for the methyl ligand, which is significantly low-field shifted when compared to the signal of the monocationic λ^4-trifluorosulfanyl complex **6'** ($\Delta\delta = 24.6$ ppm). The coupling constant to rhodium is $^1J_{C,Rh} = 24$ Hz.

Crystals of **8b** were examined by single X-ray diffraction analysis to determine the structure in the solid state (Figure 7). There is a disorder of the AsF_6^- anions as well as the SF_2 ligand, which does not allow for any discussion of the S–F bond lengths. The cation exhibits a slightly distorted square-pyramidal coordination geometry at the rhodium atom with the SF_2 ligand located in a *trans* position to the ether function of the phosphine ligand with an O–Rh–S angle of 175.5(2)°. The Rh1–S1 bond of 2.126(4) Å is slighthorter when compared to the corresponding bond length in the SF_3 complex **6**. No short contacts between the sulfur atom S1 and any fluorine atom of AsF_6^- are apparent. The minimum structure of the cation [Rh(Me)(SF_2)(^{tBu}xanPOP)]$^+$ was also determined by DFT methods (Figure 8). The sulfur-fluorine bonds are calculated to be 1.604 Å and 1.609 Å.

SF_3 group containing compounds can be oxidized by various methods to access SF_5 or SF_4Cl moieties.[16] For instance, it has been shown that trichloroisocyanuric acid (TClCA) can be used for an oxidation of disulfides to access after subsequent fluorination SF_5 groups.[16v,w,17] In contrast, treatment of **6** with 10 equiv. of TClCA in acetonitrile-d_3 led within 16 h to the formation of [Rh(F)(Cl)(SF_2)(^{tBu}xanPOP)][Cl] (**2b**), in which the cation is probably stabilized by chloride as counter anion (Scheme 3). In addition, the ^{31}P{^{1}H} and ^{19}F NMR data reveal the presence of a cationic Rh^{III}-complex (30%) and a Rh^{III}-fluorido complex (11%) together with five other minor products (less than 3%) (Supporting Information, Figures S30 and S31). Furthermore, the formation of SF_5Cl was detected by ^{19}F NMR spectroscopy. The ^{1}H NMR spectrum reveals the generation of CH_3Cl ($\delta = 3.01$ ppm, satellites: doublet, $^1J_{H,C} = 150.4$ Hz). Its resonance correlates in a ^{1}H,^{13}C-HMQC NMR spectrum with a ^{13}C signal at $\delta = 26.4$ ppm.[18]

The ^{31}P{^{1}H} NMR spectrum of **2b** at room temperature shows a doublet of triplets of doublets at $\delta = 69.6$ ppm with couplings to the metal center ($^1J_{P,Rh} = 77$ Hz), the two fluorine atoms of the SF_2 ligand ($^3J_{P,F} = 28$ Hz) and to the fluorido ligand ($^2J_{P,F} = 6$ Hz). The coupling constant between phosphorus and the fluorido ligand suggests that the fluorido ligand is located in a *cis* position to the ether function of the ^{tBu}xanPOP ligand.[8] The

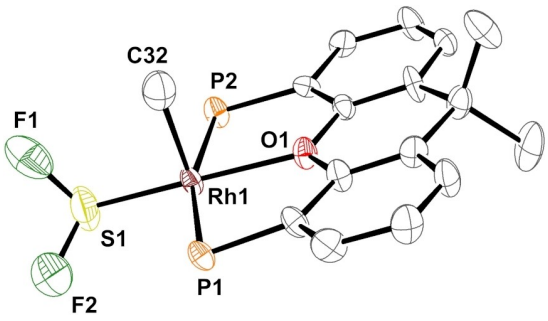

Figure 7. Structure of the cation in [Rh(Me)(SF_2)(^{tBu}xanPOP)][AsF_6]$_2$ (**8b**, ORTEP, ellipsoids are set at 50% probability. All hydrogen atoms, the *t*Bu groups as well as the AsF_6^- anions have been omitted for clarity. Selected distances [Å] and bond angles [°]: Rh1–P1 2.414(3), Rh1–P2 2.398(3), Rh1–O1 2.166(7), Rh1–C32 2.044(15), Rh1–S1 2.126(4), P1–Rh1–P2 164.56(10), S1–Rh1–O1 175.5(2), C32–Rh1–O1 87.9(4), C32–Rh1–P1 89.4(4), C32–Rh1–P2 94.0(4), C32–Rh1–S1a 95.0(4), P1–Rh1–O1 82.5(2), P2–Rh1–O1 82.6(2), S1–Rh1–P1 100.90(13), S1–Rh1–P2 93.81(14), F1–S1–Rh1 109.5(4), F2–S1–Rh1 114.7(5), F2–S1–F1 93.4(6).

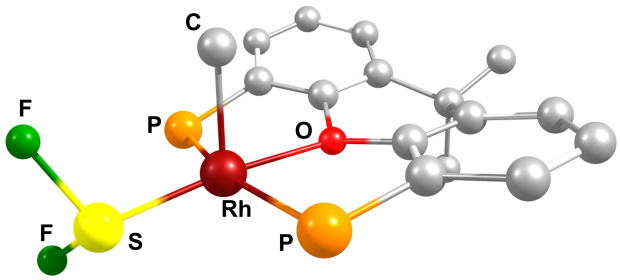

Figure 8. DFT optimized structure of the [Rh(Me)(SF_2)(^{tBu}xanPOP)]$^+$ cation; all hydrogen atoms as well as the *t*Bu groups have been omitted for clarity. B3LYP/cc-pvdz with Grimme D3 dispersion correction including Becke-Jones damping (RECP with corresponding cc-pvtz basis set for Rh).

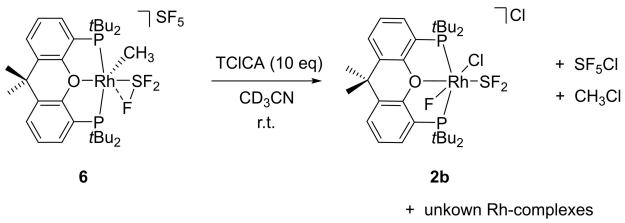

Scheme 3. Formation of [Rh(F)(Cl)(SF_2)(^{tBu}xanPOP)][Cl] (**2b**) together with the generation of SF_5Cl and CH_3Cl upon treatment of [Rh(Me)(SF_3)(^{tBu}xanPOP)][SF_5] (**6**) with trichloroisocyanuric acid (TClCA).

^{19}F NMR spectrum of **2b** shows two resonances at $\delta = -29.9$ and -406.5 ppm. The signal at lower field appears as a triplet of doublets of doublets ($^{3}J_{F,P} = 28$ Hz, $^{3}J_{F,F} = 19$ Hz, $^{2}J_{F,Rh} = 12$ Hz) and can be assigned to the sulfur-bound fluorine atoms of the SF_2 ligand. The coupling constants are consistent with these of other cationic SF_2 transition metal complexes.[4a,e,f,i] The broad doublet of triplets ($^{2}J_{F,Rh} = 176$ Hz $^{3}J_{F,F} = 20$ Hz) at high field can be attributed to a metal-bound fluorine atom and shows couplings to rhodium and the fluorine atoms bound to the SF_2 ligand, which is also confirmed by ^{19}F,^{19}F-COSY NMR spectroscopy (Supporting Information, Figure S33).[4g,7]

The oxidation with TClCA can formally be described by oxidative chlorination steps of the SF_5^- anion as well as the (anionic) CH_3 ligand. At the same time chlorination of the Rh complex occurred to give the cation [Rh(F)(Cl)(SF_2)(^{tBu}xanPOP)] and chloride as counter anion. A concomitant fluoride migration from the SF_3 ligand to the metal center results in the generation of the SF_2 fluorido complex **2b**.

Conclusion

In conclusion, rhodium ^{tBu}xanPOP complexes allow for the synthesis of SF_2 and SF_3 complexes. A unique cationic SF_3 complex [Rh(Me)(SF_3)(^{tBu}xanPOP)][SF_5] (**6**) was synthesized which displays an additional Rh–F interaction in the solid state and in solution at low temperature. A SF_3 complex has not been characterized crystallographically before. A corresponding chloride complex is not accessible as fluoride migrates to the metal center to give [Rh(F)(Cl)(SF_2)(^{tBu}xanPOP)][SF_5] (**2a**). Abstraction of fluoride from **6** with BF_3 leads to a dicationic SF_2 species. TClCA does not lead to the oxidation of the λ^4-trifluorosulfanyl ligand, but to chlorination of the SF_5^- anion and methyl ligand.

Experimental Section

Full details of experimental procedures, complex synthesis and characterisation, NMR data, IR data and crystallographic data as well as computational details can be found in the Supporting Information.

Deposition Numbers 2113737 (for 4), 2113738 (for 6), 2113739 (for 5), 2113740 (for 8b), 2113741 (for 7·C4H8O), 2120896 (for 3) contain the supplementary crystallographic data for this paper. These data are provided free of charge by the joint Cambridge Crystallographic Data Centre and Fachinformationszentrum Karlsruhe Access Structures service."

Acknowledgements

We acknowledge the DFG (Deutsche Forschungsgemeinschaft) for financial support (BR 2065/10-2). Open Access funding enabled and organized by Projekt DEAL.

Conflict of Interest

The authors declare no conflict of interest.

Data Availability Statement

The data that support the findings of this study are available in the supplementary material of this article.

Keywords: fluorido complexes · rhodium · S–F activation · sulfur fluorides · sulfur tetrafluoride

[1] a) R. E. Banks, in *Fluorine chemistry at the millennium fascinated by fluorine*, Elsevier, Amsterdam, New York, **2000**; b) J.-P. Bégué, D. Bonnet-Delpon, in *Bioorganic and Medicinal Chemistry of Fluorine*, Wiley-VCH, Hoboken, **2007**; c) J. A. Gladysz, D. P. Curran, I. T. Horvath, in *Handbook of Fluorous Chemistry*, Wiley-VCH, Weinheim, **2004**; d) A. Haupt, in *Organic and inorganic fluorine chemistry:methods and applications*, de Gruyter, Berlin, Boston, **2021**; e) P. Kirsch, in *Modern fluoroorganic chemistry: synthesis, reactivity, applications*, Wiley-VCH, Weinheim, **2013**.
[2] a) M. R. C. Gerstenberger, A. Haas, *Angew. Chem. Int. Ed. Engl.* **1981**, *20*, 647–667; *Angew. Chem.* **1981**, *93*, 659–680; b) C. Ni, M. Hu, J. Hu, *Chem. Rev.* **2015**, *115*, 765–825; c) K. Matsumoto, M. Gerken, *Dalton Trans.* **2021**, *50*, 12791–12799.
[3] a) G. S. Lal, G. P. Pez, R. J. Pesaresi, F. M. Prozonic, H. Cheng, *J. Org. Chem.* **1999**, *64*, 7048–7054; b) W. J. Middleton, *J. Org. Chem.* **2002**, *40*, 574–578; c) J. n. M. Shreeve, R. P. Singh, *Synthesis* **2002**, 2561–2578; d) T. Umemoto, R. P. Singh, Y. Xu, N. Saito, *J. Am. Chem. Soc.* **2010**, *132*, 18199–18205; e) W. Xu, H. Martinez, W. R. Dolbier, *J. Fluorine Chem.* **2011**, *132*, 482–488.
[4] a) R. W. Cockman, E. A. V. Ebsworth, J. H. Holloway, *J. Am. Chem. Soc.* **1987**, *109*, 2194–2195; b) P. Watson, Dissertation thesis, University of Edinburgh (Edinburgh), **1990**; c) H. M. Murdoch, Dissertation thesis, University of Edinburgh (Edinburgh), **1991**; d) R. W. Cockman, E. A. V. Ebsworth, J. H. Holloway, H. Murdoch, N. Robertson, P. G. Watson, in *Inorganic Fluorine Chemistry, Vol. 555* (Eds.: J. S. Thrasher, S. H. Strauss), American Chemical Society, **1994**, pp. 326–337; e) C. Berg, T. Braun, M. Ahrens, P. Wittwer, R. Herrmann, *Angew. Chem. Int. Ed.* **2017**, *56*, 4300–4304; *Angew. Chem.* **2017**, *129*, 4364–4368; f) C. Berg, N. Pfister, T. Braun, B. Braun-Cula, *Chem. Eur. J.* **2018**, *24*, 7985–7990; g) N. Pfister, T. Braun, P. Wittwer, M. Ahrens, *Z. Anorg. Allg. Chem.* **2018**, *644*, 1064–1070; h) R. Jaeger, M. Talavera, T. Braun, *J. Fluorine Chem.* **2021**, *247*; i) N. Pfister, M. Bui, T. Braun, P. Wittwer, M. Ahrens, *Z. Anorg. Allg. Chem.* **2020**, *646*, 808–815; j) D. Dirican, N. Pfister, M. Wozniak, T. Braun, *Chem. Eur. J.* **2020**, *26*, 6945–6963; k) D. Dirican, M. Talavera, T. Braun, *Chem. Eur. J.* **2021**, *27*, 17707–17712.
[5] X. Gao, N. Li, R. B. King, *Inorg. Chem.* **2014**, *53*, 12635–12642.
[6] a) F. Buss, C. Muck-Lichtenfeld, P. Mehlmann, F. Dielmann, *Angew. Chem. Int. Ed.* **2018**, *57*, 4951–4955; *Angew. Chem.* **2018**, *130*, 5045–5049; b) M. Rueping, P. Nikolaienko, Y. Lebedev, A. Adams, *Green Chem.* **2017**, *19*, 2571–2575.
[7] a) H. Baumgarth, G. Meier, T. Braun, B. Braun-Cula, *Eur. J. Inorg. Chem.* **2016**, *2016*, 4565–4572; b) N. Bramananthan, M. Carmona, J. P. Lowe, M. F. Mahon, R. C. Poulten, M. K. Whittlesey, *Organometallics* **2014**, *33*, 1986–1995; c) T. Braun, D. Noveski, B. Neumann, H.-G. Stammler, *Angew. Chem. Int. Ed.* **2002**, *41*, 2745–2748; *Angew. Chem.* **2002**, *114*, 2870–2873; d) R. R. Burch, R. L. Harlow, S. D. Ittel, *Organometallics* **1987**, *6*, 982–987; e) B. Callejas-Gaspar, M. Laubender, H. Werner, *J. Organomet. Chem.* **2003**, *684*, 144–152; f) J. Gil-Rubio, J. Vicente, *Dalton Trans.* **2015**, *44*, 19432–19442; g) J. Gil-Rubio, B. Weberndörfer, H. Werner, *J. Chem. Soc. Dalton Trans.* **1999**, 1437–1444; h) B. T. Heaton, J. A. Iggo, C. Jacob, H. Blanchard, M. B. Hursthouse, I. Ghatak, M. E. Harman, R. G. Somerville, W. Heggie, P. R. Page, I. Villax, *J. Chem. Soc. Dalton Trans.* **1992**, 2533–2537; i) S. A. Macgregor, D. C. Roe, W. J. Marshall, K. M. Bloch, V. I. Bakhmutov, V. V. Grushin, *J. Am. Chem. Soc.* **2005**, *127*, 15304–15321; j) A. Meiswinkel, H. Werner, *Inorg. Chim. Acta* **2004**, *357*, 2855–2862; k) F. Nahra, M. Brill, A. Gómez-Herrera, C. S. J. Cazin, S. P. Nolan, *Coord. Chem. Rev.* **2016**, *307*, 65–80; l) D. Noveski, T. Braun, S. Krückemeier, *J. Fluorine Chem.* **2004**, *125*, 959–966; m) D. Noveski, T. Braun, M. Schulte, B.

Neumann, H.-G. Stammler, *Dalton Trans.* **2003**, 4075–4083; n) C. Segarra, E. Mas-Marzá, J. P. Lowe, M. F. Mahon, R. C. Poulten, M. K. Whittlesey, *Organometallics* **2012**, *31*, 8584–8590; o) M. Teltewskoi, J. A. A. Panetier, S. A. A. Macgregor, T. Braun, *Angew. Chem. Int. Ed.* **2010**, *49*, 3947–3951; *Angew. Chem.* **2010**, *122*, 4039–4043; p) B. J. Truscott, F. Nahra, A. M. Z. Slawin, D. B. Cordes, S. P. Nolan, *Chem. Commun.* **2015**, *51*, 62–65; q) H. L. M. van Gaal, F. L. A. van den Bekerom, *J. Organomet. Chem.* **1977**, *134*, 237–248; r) J. Vicente, J. Gil-Rubio, D. Bautista, A. Sironi, N. Masciocchi, *Inorg. Chem.* **2004**, *43*, 5665–5675; s) L. Zamostna, T. Braun, B. Braun, *Angew. Chem. Int. Ed.* **2014**, *53*, 2745–2749; *Angew. Chem.* **2014**, *126*, 2783–2787.

[8] M. Wozniak, T. Braun, M. Ahrens, B. Braun-Cula, P. Wittwer, R. Herrmann, R. Laubenstein, *Organometallics* **2018**, *37*, 821–828.

[9] a) M. C. Haibach, D. Y. Wang, T. J. Emge, K. Krogh-Jespersen, A. S. Goldman, *Chem. Sci.* **2013**, *4*, 3683–3692; b) S. G. Curto, M. A. Esteruelas, M. Oliván, E. Oñate, A. Vélez, *Organometallics* **2017**, *36*, 114–128; c) M. A. Esteruelas, M. Oliván, A. Vélez, *Organometallics* **2015**, *34*, 1911–1924; d) M. A. Esteruelas, M. Oliván, A. Vélez, *Inorg. Chem.* **2013**, *52*, 5339–5349; e) M. A. Esteruelas, M. Olivan, A. Velez, *Inorg. Chem.* **2013**, *52*, 12108–12119; f) S. G. Curto, M. A. Esteruelas, M. Oliván, E. Oñate, *Organometallics* **2019**, *38*, 2062–2074.

[10] a) J. Bittner, J. Fuchs, K. Seppelt, *Z. Anorg. Allg. Chem.* **1988**, *557*, 182–190; b) J. T. Goettel, N. Kostiuk, M. Gerken, *Angew. Chem. Int. Ed.* **2013**, *52*, 8037–8040; *Angew. Chem.* **2013**, *125*, 8195–8198; c) N. Kostiuk, J. T. Goettel, M. Gerken, *Inorg. Chem.* **2020**, *59*, 8620–8628; d) R. Tunder, B. Siegel, *J. Inorg. Nucl. Chem.* **1963**, *25*, 1097–1098; e) R. F. Weitkamp, B. Neumann, H. G. Stammler, B. Hoge, *Chem. Eur. J.* **2021**, *27*, 6465–6478.

[11] P. Ren, S. D. Pike, I. Pernik, A. S. Weller, M. C. Willis, *Organometallics* **2015**, *34*, 711–723.

[12] a) G. M. Adams, A. L. Colebatch, J. T. Skornia, A. I. McKay, H. C. Johnson, G. C. Lloyd Jones, S. A. Macgregor, N. A. Beattie, A. S. Weller, *J. Am. Chem. Soc.* **2018**, *140*, 1481–1495; b) A. Conkie, E. A. V. Ebsworth, R. A. Mayo, S. Moreton, *J. Chem. Soc. Dalton Trans.* **1992**, 2951–2954.

[13] M. Talavera, T. Braun, *Chem. Eur. J.* **2021**, *27*, 11926–11934.

[14] a) P. Basnet, S. Kc, R. K. Dhungana, B. Shrestha, T. J. Boyle, R. Giri, *J. Am. Chem. Soc.* **2018**, *140*, 15586–15590; b) M. Finze, E. Bernhardt, M. Zahres, H. Willner, *Inorg. Chem.* **2004**, *43*, 490–505.

[15] W. Gombler, J. Schaebs, H. Willner, *Inorg. Chem.* **2002**, *29*, 2697–2698.

[16] a) G. A. Silvey, G. H. Cady, *J. Am. Chem. Soc.* **1952**, *74*, 5792–5793; b) F. W. Hoffmann, T. C. Simmons, R. Beck, H. Holler, T. Katz, R. Koshar, E. Larsen, J. Mulvaney, F. Rogers, B. Singleton, *J. Am. Chem. Soc.* **1957**, *79*, 3424–3429; c) W. A. Sheppard, *J. Am. Chem. Soc.* **1960**, *82*, 4751–4752; d) W. A. Sheppard, *J. Am. Chem. Soc.* **1962**, *84*, 3064–3072; e) A. F. Clifford, G. R. Zeilenga, *Inorg. Chem.* **1969**, *8*, 979–980; f) T. Abe, S. Nagase, K. Kodaira, H. Baba, *Bull. Chem. Soc. Jpn.* **1970**, *43*, 1812–1816; g) A. Waterfeld, R. Mews, *Angew. Chem. Int. Ed. Engl.* **1981**, *20*, 1017–1017; *Angew. Chem.* **1981**, *93*, 1075–1075; h) A. Waterfeld, R. Mews, *J. Fluorine Chem.* **1983**, *23*, 325–330; i) X. Ou, A. F. Janzen, *J. Fluorine Chem.* **2000**, *101*, 279–283; j) A. M. Sipyagin, C. P. Bateman, Y.-T. Tan, J. S. Thrasher, *J. Fluorine Chem.* **2001**, *112*, 287–295; k) L. A. Shimp, R. J. Lagow, *Inorg. Chem.* **2002**, *16*, 2974–2975; l) P. J. Crowley, G. Mitchell, R. Salmon, P. A. Worthington, *Chimia* **2004**, *58*, 138–142; m) A. M. Sipyagin, V. S. Enshov, S. A. Kashtanov, C. P. Bateman, B. D. Mullen, Y.-T. Tan, J. S. Thrasher, *J. Fluorine Chem.* **2004**, *125*, 1305–1316; n) P. Kirsch, A. Hahn, Wiley Online Library, *Eur. J. Org. Chem.* **2005**, 3095–3100; o) T. Umemoto, L. M. Garrick, N. Saito, *Beilstein J. Org. Chem.* **2012**, *8*, 461–471; p) K. Lummer, M. V. Ponomarenko, G.-V. Röschenthaler, M. Bremer, P. Beier, *J. Fluorine Chem.* **2014**, *157*, 79–83; q) A. M. Sipyagin, C. P. Bateman, A. V. Matsev, A. Waterfeld, R. E. Jilek, C. D. Key, G. J. Szulczewski, J. S. Thrasher, *J. Fluorine Chem.* **2014**, *167*, 203–210; r) O. S. Kanishchev, W. R. Dolbier, Jr., *Angew. Chem. Int. Ed.* **2015**, *54*, 280–284; *Angew. Chem.* **2015**, *127*, 282–286; s) P. R. Savoie, J. T. Welch, *Chem. Rev.* **2015**, *115*, 1130–1190; t) B. Cui, M. Kosobokov, K. Matsuzaki, E. Tokunaga, N. Shibata, *Chem. Commun.* **2017**, *53*, 5997–6000; u) J. Ajenjo, B. Klepetarova, M. Greenhall, D. Bim, M. Culka, L. Rulisek, P. Beier, *Chem. Eur. J.* **2019**, *25*, 11375–11382; v) F. Brüning, C. R. Pitts, J. Kalim, D. Bornemann, C. Ghiazza, J. Montmollin, N. Trapp, T. Billard, A. Togni, *Angew. Chem. Int. Ed.* **2019**, *58*, 18937–18941; *Angew. Chem.* **2019**, *131*, 19113–19117; w) C. R. Pitts, D. Bornemann, P. Liebing, N. Santschi, A. Togni, *Angew. Chem. Int. Ed.* **2019**, *58*, 1950–1954; *Angew. Chem.* **2019**, *131*, 1970–1974; x) O. I. Guzyr, V. N. Kozel, E. B. Rusanov, A. B. Rozhenko, V. N. Fetyukhin, Y. G. Shermolovich, *J. Fluorine Chem.* **2020**, *239*.

[17] J. Y. Shou, X. H. Xu, F. L. Qing, *Angew. Chem. Int. Ed.* **2021**, *60*, 15271–15275; *Angew. Chem.* **2021**, *133*, 15399–15403.

[18] a) M. Burchner, A. M. Erle, H. Scherer, I. Krossing, *Chem. Eur. J.* **2012**, *18*, 2254–2262; b) A. M. Schrader, A. L. Schroll, G. Barany, *J. Org. Chem.* **2011**, *76*, 7882–7892; c) C. Wakai, S. Morooka, N. Matubayasi, M. Nakahara, *Chem. Lett.* **2004**, *33*, 302–303; d) K. B. Wiberg, W. E. Pratt, W. F. Bailey, *J. Org. Chem.* **2002**, *45*, 4936–4947.

Manuscript received: February 25, 2022
Accepted manuscript online: April 14, 2022
Version of record online: May 4, 2022